Asian Journal of Chemistry; Vol. 37, No. 12 (2025), 3136-3146
ASIAN JOURNAL OF CHEMISTRY
https://doi.org/10.14233/ajchem.2025.34341

Design, Synthesis, *in vitro* Anticancer Activity, Topoisomerase-I Inhibition and DNA Binding Studies of Substituted Carbazole Semicarbazone Derivatives

NITIN KUMAR*, NEETIKA LAL, VISHAL NEMAYSH and PRATIBHA MEHTA LUTHRA

Neuropharmaceutical Chemistry Research Laboratory, Dr. B.R. Ambedkar Center for Biomedical Research, University of Delhi, Delhi-110007, India

*Corresponding author: E-mail: nitinvishnoi@gmail.com

Received: 26 June 2025 *Accepted*: 11 November 2025 *Published online*: 30 November 2025 AJC-22205

Glioblastoma multiforme (GBM) is the most aggressive and deadly form of brain tumor in adults. In the search for more effective anticancer agents, tricyclic compounds such as carbazole derivatives have garnered considerable attention. This study aims to design and synthesize new substituted carbazole semicarbazone derivatives and evaluate their *in vitro* anticancer profile (IC_{50}) on U87 MG glioma cell line based on MTT assay and DNA binding mechanism of one potent cytotoxic compound with calf thymus DNA *via* spectroscopic methods, topoisomerase assay and *in silico* approach. Reaction of 6-substituted carbazole-3-carbaldehyde with semicarbazide in 1:1 ratio reflux in ethanol gave 6-substituted carbazole semicarbazone derivatives and their structure elucidated by their melting point, NMR, FT-IR, HRMS spectroscopy. DNA binding studies of one potent cytotoxic carbazole derivative with *ct*-DNA (calf-thymus) in physiological buffer (pH 7.4) carried *via* various spectroscopic techniques like electronic absorption, circular dichroism (CD), viscosity test, topoisomerase assay and computational method. Two carbazole semicarbazone derivatives [(6-bromo-1,4-dimethyl-9*H*-carbazol-3-yl)-methylideneamino]urea (**21**) and [(6-methoxy-1,4-dimethyl-9*H*-carbazol-3-yl)methylideneamino]urea (**22**) found the best anticancer activities against the U87MG glioma cell line with the 50% inhibitory concentration (IC_{50}) values IC_{50} = 23.3 ± 4 μM and 13.82 ± 3.86 μM, respectively also which even better than standard drug temozolomide (IC_{50} = 100 μM). Spectroscopic studies (UV absorption, circular dichroism), viscosity test and molecular docking analysis confirmed that carbazole semicarbazone (**22**) has groove binding mode with *ct*-DNA. Only topoisomerase assay, compound **22** showed groove binding mode interaction concentration dependent manner. These carbazole semicarbazone derivatives demonstrated potent anticancer activity against the U87MG glioma cell line. Spectroscopic analyses, viscosity test and molecular docking confirmed that compound **22** interacts with *ct*-DNA *via* a groove binding mode. Moreover, topoisomerase inhibition assays supported this interaction in a concentration-dependent manner, suggesting that compound **22** may exert its anticancer effect through DNA-targeted mechanisms.

Keywords: Glioblastoma, Carbazoles, Semicarbazone, Topoisomerase enzyme.

INTRODUCTION

Glioblastoma multiforme (GBM) is a type IV grade tumor according to WHO classification [1-3]. After diagnosis, surgery, radiation exposure therapy and chemotherapy are main treatment option depending upon brain tumor grade [4-6]. However, survival of GBM patients only 15-16 months or less [4-6]. So, developing of new chemotherapeutic agents for treatment of GBM is urgent needed.

DNA carries essential genetic information and plays a central role in cellular processes [7]. It is also a critical target for many anticancer agents [7]. Depending on their structural features, small molecules can interact with DNA through either covalent or non-covalent binding modes [8-11]. These interactions may occur *via* a single binding mode or through mixed modes [12,13]. Investigating the interactions between drugs (or other chemical compounds) and DNA is valuable for the development of novel anticancer therapeutics and for elucidating their mechanisms of action and potential genotoxicity [14].

Carbazole derivatives play a significant role in various biological activities, making them highly attractive scaffolds for medicinal chemists in the pursuit of novel and effective anticancer agents [15-20]. Reported substituted carbazole guanidine derivatives (**1**) showed potential *in vitro* cytotoxicity against HL-60 cell line (Fig. 1) [21]. 1,4-Dimethyl-9-*H*-carbazole containing *N*-(3,4,5-trimethoxyphenyl)ureido group (**2**)

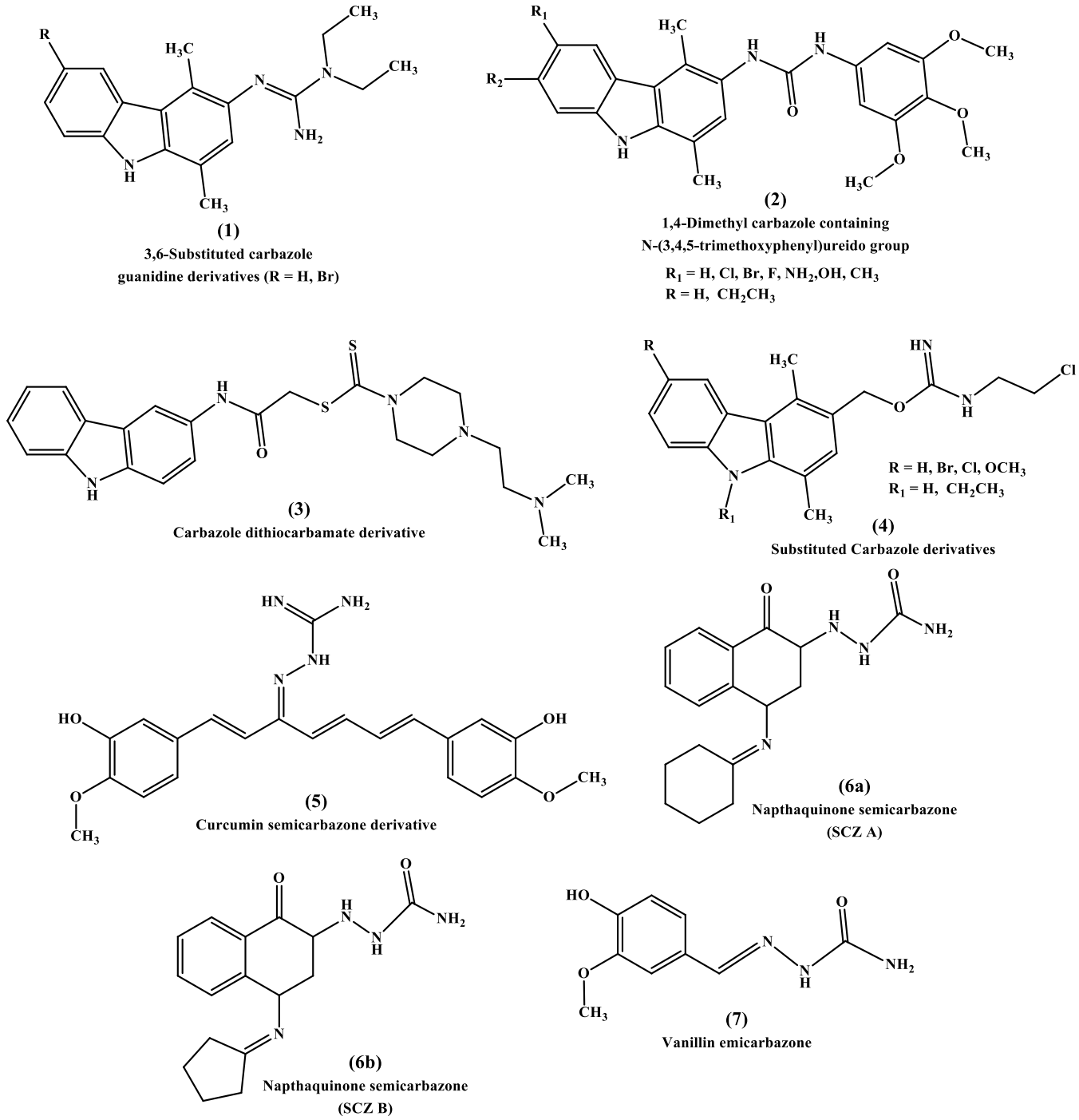

Fig. 1. Structure of some important 3, 6 and N-9 substituted carbazole scaffold based potential molecules (**1-4**). Structure of curcumin semicarbazone (**5**), 4-cycloalkylidine amino cycloalkylidineamino 1,2-naphthoquinone semicarbazone (**6**) and (**6B**), vanillin semicarbazone (**7**)

showed potential *in vitro* cytotoxicity (IC_{50}) activity on KB and HL-60 cell line also good tubulin polymerization inhibitory activity (Fig. 1) [22]. Ciftci *et al.* [23] reported carbazole dithiocarbamates derivative containing substituted piperazine (**3**) displayed potential *in vitro* cytotoxicity against C6 (glioma) cell lines.

Caruso *et al.* [21] investigated changing substitution mainly electron withdrawing group on the 6th position of carbazole scaffold linked to guanidine moiety **(1)** also found crucial role in anticancer activity on various cancer cell lines (Fig. 1) [21]. Panno *et al.* [22] group also report changing substitution on the 6th position 1,4-dimethyl-9*H*-carbazole part containing N-(3,4,5-trimethoxy phenyl)ureido group play crucial role in anticancer activity on various cancer cell lines (Fig 1). Recently, in our three published works, changing substitution either electron withdrawing or electron donating group on C6 position on carbazole scaffold was crucial for potent *in vitro* anticancer activity on U87MG cell line [21,22,24,25].

Semicarbazones contains urea functional group showed potential anticancer activities on different cancer cell lines (Fig. 2) [26-31]. Recently, our group reported the design, synthesis and anticancer evaluation of novel substituted bis-carbazole derivatives, as well as 6-substituted carbazole thiosemicarbazone derivatives (**9**), on the U87 MG glioma cell line using the MTT assay [24,32,33]. The design of the bis-carbazole compounds was inspired by the structure of ellipticine (**8**), a pyridocarbazole derivative known for its significant anticancer activity across various cancer cell lines [25,34,35]. Building on this work, we also synthesized substituted carbazole derivatives bearing a thiosemicarbazide group (**10**) (Fig. 2), which exhibited notable anticancer activity against the U87 MG glioma cell line [33]. Furthermore, recently reported N-substituted carbazole semicarbazone and thiosemicarbazone derivatives demonstrated significant antibacterial activity [36].

Several anticancer drugs currently in clinical use, such as sorafenib, carmofur and lenvatinib, incorporate thio/urea scaffolds in their structures [37]. Extensive research has shown that these compounds can interact with multiple molecular targets involved in cancer therapy. Their anticancer mechanisms of action include inhibition of angiogenesis, cell cycle arrest and inhibition of enzymes crucial to cancer progression such as topoisomerases, ATPases and dihydroorotate dehydrogenase [37-40]. Novel benzothiazole semicarbazone derivatives (Fig. 2) showed potential *in vitro* antitumor against tested four cancer cell lines (HT29, H460, A549 and MDA-MB-231) [40]. So, consider potential of carbazole and semicarbazone based derivatives on cancer cell line, we design and synthesized substituted carbazole semicarbazone derivatives and tested for *in vitro* anticancer activity on the U87 MG cell line. DNA binding studies of best cytotoxic compound **22** with *ct*-DNA was carried by various spectroscopic techniques like electronic spectroscopy, circular dichroism (CD) and further viscosity test, topoisomerase assay and docking analysis.

EXPERIMENTAL

All chemical and regents analytical were procured from Sigma Co. USA and Alpha Aesar, antibiotics and fetal bovine

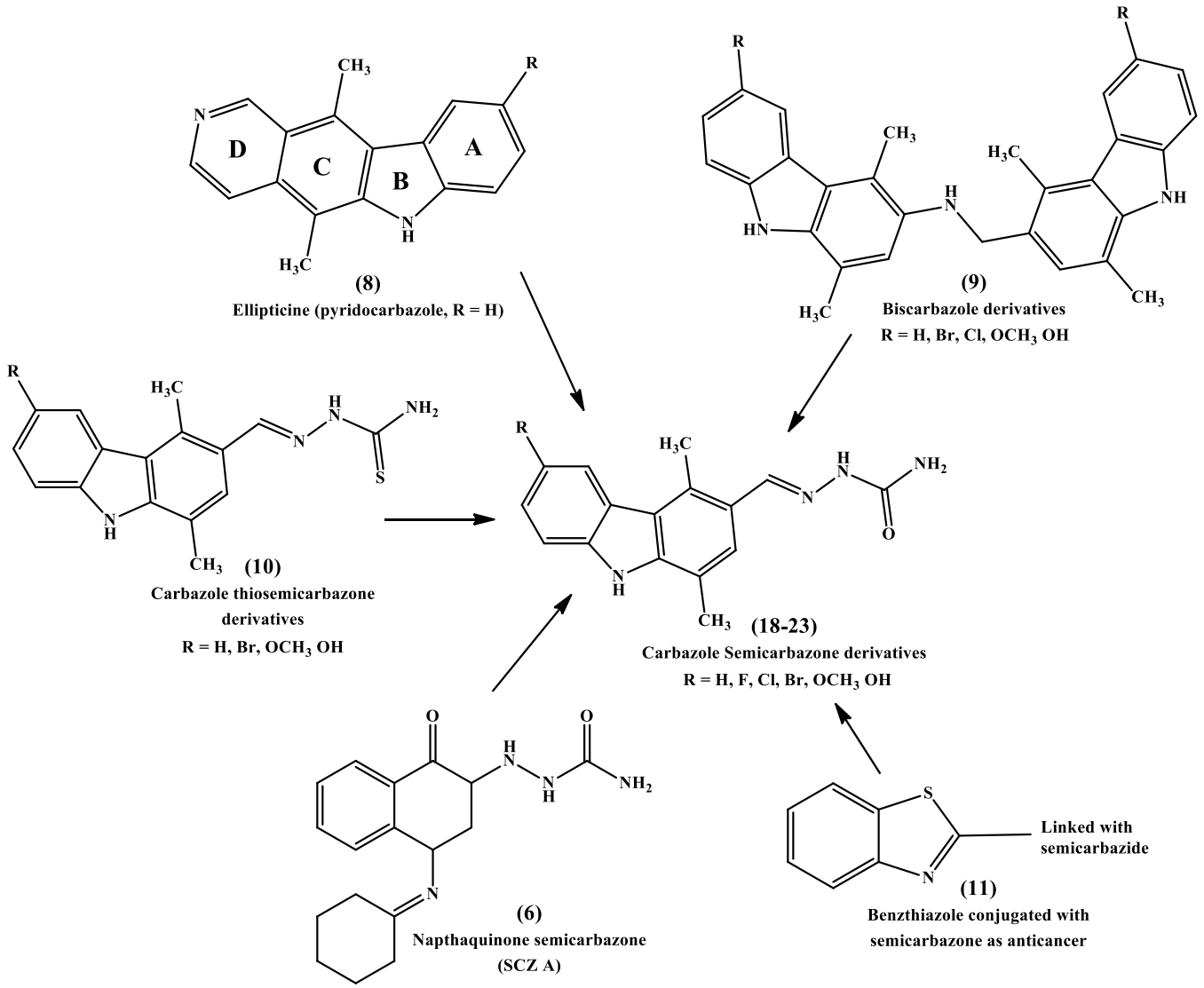

Fig. 2. Rationale of novel 6-substituted carbazole semicarbazone derivative (**18-23**) based on ellipticine (**8**), *bis*carbazole derivatives (**9**), carbazole thiosemicarbazones (**10**), napthaquinone and benzthiazole semicarbazone (**6A** and **10**)

serum (FBS) procured from Hi-Media Laboratories Ltd. TLC was taken on available Silica Gel 60 F_{254}, Merck using two TLC system 20% or 40% ethyl acetate (EA) in petroleum ether (PE), respectively. Stock solutions of *ct*-DNA were prepared in sterile water for injection gave a ratio of UV optical density (OD) reading at 260 and 280 nm (A_{260}/A_{280}) found in a range 1.8-1.9 [25,32]. DNA concentration was calculated by UV spectrophotometer by the using molar extinction coefficient value (E) (6600 M^{-1} cm^{-1}) at wavelength 260 nm [25,32]. DNA binding experiments carried out in physiological phosphate buffer (pH 7.4). The resulting compound-DNA complex solutions were incubated for 30 min before the final UV spectroscopy; CD spectra and viscosity test were recorded.

Instruments: All new synthesized compounds prepared were confirmed by melting point, infrared spectra, NMR and high-resolution mass spectra (HRMS) spectroscopy. ^{1}H NMR and ^{13}C NMR spectra were taken on Bruker Avance II and JEOL 400 MHz NMR spectrophotometer, respectively. IR data of all final carbazole derivatives were recorded by KBr dry pellets method on Perkin-Elmer instrument. Mass (HRMS) of the compounds was taken by using a Micromass, Q-TOF micro (Water) spectrophotometer. UV-visible absorption spectra were taken on a Perkin-Elmer instrument. Circular dichroism spectra were recorded using a JASCO J-810 spectropolarimeter.

Synthesis of substituted carbazole semicarbazone derivatives (18-23): Equimolar quantity of earlier prepared starting material 6-substituted carbazol-3-carbaldehyde **(12-17**) [25,32,33,36] and semicarbazide hydrochloride dissolved in ethanol were refluxed for 4-6 h [25,26]. Reaction mixture progress was checked by using two TLC system (20% or 40% EA/PE solvent (**Scheme-I**). Reaction mixture was allowed to cool and appears precipitate filtered out and washed it twice ethanol:water (2:8) three times and dried it in desiccators without further purification.

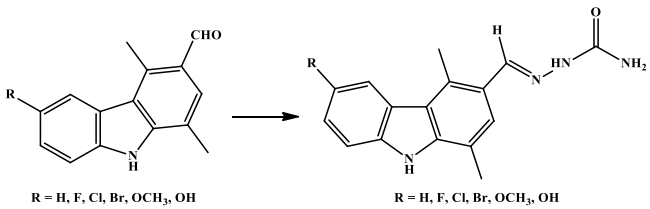

Scheme-I: Reagent and condition (A) semicarbazide hydrochloride, ethanol, reflux 4-6 h

[(1,4-Dimethyl-9*H*-carbazol-3-yl)methylideneamino]-urea (18): Yield: 80%, Light pink solid; m.p.: 260-261 ºC. IR (KBr, ν_{max}, cm^{-1}): 3430.37, 3310 (NH_2, NH), 3000, 2916.76 (aromatic aliphatic carbon), 1673.25 (C=O), 1593.43 (C=N); ^{1}H NMR (400 MHz, δ ppm): 11.50 (1H-indole N-H, brs), 10.01 (1 NH-N, brs), 8.39 (CH=N, s), 7.86 (1H, s, aromatic), 7.64 (1H, d, arom.), 7.41 (1-H, d, arom.), 7.14 (dd, 1H, arom.), 6.45 (2-NH_2, brs), 2.80 (3H, s, CH_3), 2.49 (3H, s, CH_3); ^{13}C NMR (400 MHz, δ ppm): 156.2, 142.39, 141.1, 140, 129, 127, 126, 124, 123, 119, 118.2, 110, 109, 17.15, 16.16. HRMS (ESI-Q-TOF): $C_{16}H_{16}N_4O$ $[M+H]^+$ calcd. *m/z*, 280.1324, found (*m/z*) M+1 = 281.1401.

[(6-Fluoro-1,4-dimethyl-9*H*-carbazol-3-yl)methylidene-amino]urea (19): Yield: 70%, Light pink solid. m.p.: 340-341 ºC. IR (KBr, ν_{max}, cm^{-1}): 3454.83, 3314 (NH_2, NH), 3000, 2916 (aromatic aliphatic carbon), 1694.25 (C=O), 1587.24 (C=N); ^{1}H NMR (400 MHz, δ ppm): 11.54 (1-Indole N-H br, s), 10.00 (1-NH-N, brs), 8.36 (CH=N, s), 8.14 (1H, s, aromatic), 7.92 (d, 1H, aromatic), 7.36 (1-H, d aromatic), 7.30 (d, 1H, aromatic), 6.41 (2-NH_2 br, s), 2.78 (3H, s), 2.49 (3-H, s). HRMS (ESI-Q-TOF): $C_{16}H_{15}N_4OF$ $[M+H]^+$ calcd. *m/z*, 298.1229, found (*m/z*) M+1 = 299.1315.

[(6-Chloro-1,4-dimethyl-9*H*-carbazol-3-yl)methylide-neamino]urea (20): Yield: 80%, pinkish solid; m.p.: 317-318 ºC; IR (KBr, ν_{max}, cm^{-1}): 3454.83 & 3300 (NH), 3000, 2980 (aromatic aliphatic carbon), 1694.25 (C=O), 1587.24 (C=N); ^{1}H NMR (400 MHz, δ ppm): 11.60 (1-Indole N-H br, s), 10.01 (1-NH-N, brs), 8.35 (CH=N, s), 8.10 (1H, s, aromatic), 7.90 (1H, d aromatic), 7.40 (d, 1-H, aromatic), 7.34 (d, 1H, aromatic), 6.37 (2-NH_2, brs), 2.77 (3H, s), 2.49 (3-H, s); HRMS (ESI-Q-TOF): $C_{16}H_{15}N_4OCl$ $[M + H]^+$ calcd. *m/z*, 314.0934, found (*m/z*) M +1 = 315.1009.

[(6-Bromo-1,4-dimethyl-9*H*-carbazol-3-yl)methylid-eneamino]urea (21): Yield: 80%, Light pinkish solid; m.p.: 320-321 ºC. IR (KBr, ν_{max}, cm^{-1}): 3454.83 & 3293.68 (NH_2, NH), 3000 , 2891 (aromatic, aliphatic carbon), 1694.25 (C= O), 1587.24 (C=N); ^{1}H NMR (400 MHz, δ ppm): 11.50 (s, 1H, -NH), 11.20 (s, indole NH), 8.37 (s, 1H, -CH=), 8.1 (s, 1H, arom.), 7.50 (d, 1H, aromatic), 7.42 (d, 1H, aromatic), 7.24 (d, 1H, aromatic), 6.5 (s, 2H, broad, -NH_2); 2.8 (s, 3H, -CH_3), 2.5 (s, 3H, -CH_3); ^{13}C NMR (400 MHz, δ ppm): 156.70, 146, 143, 142, 140.20, 130.4, 129.1, 127, 124.2, 125.50, 122, 121, 118, 114, 17.16, 15.80. HRMS (ESI-Q-TOF): $C_{16}H_{15}BrN_4S$ $[M+H]^+$ calcd. *m/z*, 358.0429, found (*m/z*) M+1 = 359.0501. Anal. Calcd. (found) % for $C_{16}H_{15}N_4OBr$ (*m.w.* 358.0429): C, 53.50 (53.80); H, 4.21 (3.98); N, 15.60 (15.71).

[(6-Methoxy-1,4-dimethyl-9*H*-carbazol-3-yl)methyli-deneamino]urea (22): Yield: 80%, Light pinkish solid; m.p.: 308-309 ºC. IR (KBr, ν_{max}, cm^{-1}): 3435.53, 3312.55 (NH_2, NH), 3000, 2830.37 (aromatic, aliphatic carbon), 1673.60 (C=O), 1595.48 (C=N); ^{1}H NMR (400 MHz, δ ppm): 11.18 (indole N-H, br, s), 9.98 (1-NH-N, brs), 8.41 (CH=N, s), 7.88 (1H, aromatic), 7.66 (1H, d, aromatic), 7.42 (d, 1H, aromatic), 7.04 (d, 1H, aromatic), 6.40 (2H, 2-NH_2, brs), 3.84 (3H, s, OCH_3), 2.80 (3H, s, CH_3), 2.49 (3H, s, CH_3); ^{13}C NMR (400 MHz, δ ppm): 157.37, 153.50, 140.69, 139.61, 135.34, 129.81, 124.26, 124.17, 123.28, 121.04, 118.53, 114.05, 112.15, 106.20, 56.49, 17.12, 15.46. HRMS (ESI-Q-TOF): $C_{17}H_{18}N_4O_2$ $[M + H]^+$ calcd. *m/z*, 310.1429, found (*m/z*) M+1 = 311.1503. Anal. calcd. (found) % for $C_{17}H_{19}N_4O_2$ (*m.w.* 310.1429): C, 65.79 (65.96); H, 5.85 (5.71); N, 18.05 (17.92).

[(6-Hydroxy-1,4-dimethyl-9*H*-carbazol-3-yl)methyli-deneamino]urea (23): Yield: 80%, Pinkish solid, m.p.: 338-339 ºC. IR (KBr, ν_{max}, cm^{-1}): 3420.83, 3280 (NH_2, NH), 3000, 2980 (aromatic, aliphatic carbon), 1680.25 (C=O), 1578.24 (C=N). ^{1}H NMR (400 MHz, δ ppm): 10.99 (1-indole N-H, br s), 9.94 (1-NH-N, br s), 8.89 (1-OH, s), 8.37 (CH=N, s), 7.82 (1H, arom.), 7.53 (1H, d, arom.), 7.32 (1H, d, arom.), 6.88 (m, 1H, arom.), 6.36 (2-NH_2, brs), 2.77 (3H, s), 2.49 (3H, s). ^{13}C NMR (400 MHz, δ ppm): 156.86, 150.51, 140.16, 139.23, 133.98, 129.20, 124.03, 123.48, 122.50, 120.47, 117.86, 114.12, 111.42, 107.36, 16.60, 14.87. HRMS (ESI-Q-TOF): $C_{16}H_{16}N_4O$ $[M + H]^+$ calcd. *m/z*, 296.1273, found *m/z* M+1 = 297.1346.

ADME and toxicity prediction studies: The ADME prediction studies were carried out online by free Molinspiration software available online. The toxicity studies were carried out online by ProTox II software.

Cell lines and culture conditions: Human glioma U87 MG cells or HEK293T cells were cultured in DMEM with FBS 10% (v/v), antibiotic and antimycotic solution. Cells were grown in a humidified incubator at 37 ºC supplemented with 5% CO_2 and 95% air during the night. The subsequent day cells adhere to the culture matrix were treated with or without compounds **18-23** for 24 h [25,40].

Cell viability MTT assay: Treatment of cells (5×10^3 U87) with various concentrations (1 μM to 300 μM) of compounds **18-23** for 24 h time. Cytotoxicity experiments were performed in triplicate (all six final compounds). The IC_{50} value for the compounds **18-23** was calculated *via* percent survival formula. All statistical calculations for final carbazole compounds carried with the standard deviation formula. GraphPad Prism 5.0 for windows was used for calculating the IC_{50} values and error by non-linear regression analysis (GraphPad Prism software) [25,32]:

$$\sigma = \sqrt{\frac{\sum (x_i - \mu)^2}{N}}$$

σ = compound standard deviation, μ = average mean value of the compound, x_i = value in the data set, N = number of data points in sample.

Electronic absorption spectral study: A fixed concentration of compound **22** (10 μM) was used, while the concentration of *ct*-DNA was incrementally increased from 0 to 20 μM and the corresponding UV spectra were recorded [25,32].

Circular dichroism spectral study: Fixed concentration of *ct*-DNA (10 μM) with incremental concentrations of compound **22** (0-20 μM) was scanned (220-350 nm), in 1 cm quartz cuvette and then the corresponding UV spectra were recorded [14,25].

Viscosity test: Viscosity test was performed on an Ostwald Type viscometer with previous reported papers [25,39]. Flow time was calculated. Graph were plot between $(\eta/\eta_o)^{1/3}$ *versus* binding ratio (R = compound **22**/*ct*-DNA]. The calculations were performed according to the reported methods [14,25].

Evaluate of topoisomerase enzyme activity

Standard human topoisomerase I relaxation and DNA unwinding assay: Supercoiled/relaxed plasmid DNA (250 ng) was incubated with the compound **22** (0.01-100 μM) and purified human topoisomerase I (HuTOPI) (TopoGEN, Inc.) in the reaction buffer (10 mM, Tris–HCl, pH 7.9, 150 mM NaCl, 0.1% BSA, 0.1 mM spermidine and 5% glycerol, final volume 20 μL) at 37 ºC for 30 min. After incubation, the reactions were impeded by the addition of pre-warmed stop solution (10% SDS/0.5M EDTA/0.25% bromophenol blue) and electrophoresis was carried in a horizontal 1% agarose gel in tris-borate-EDTA buffer at 1.5 V cm^{-1} for 14-16 h at room temperature. The gels were stained with ethidium bromide (0.5 μg/mL), de-stained in water and take photograph under ultraviolet illumination in a Chemi Doc It^2 Imager [25,32].

DNA unwinding assay: The ability of compound **22** to bind to DNA either minor groove or intercalation was studied with the topoisomerase I unwinding assay. The unwinding assay was carried with 250 ng of pHOT1plasmid DNA in the presence or absence of compound **22**, ethidium bromide and Hoechst 33342 in 20 μL of reaction mixture. Relaxed DNA was prepared by treating the super coiled plasmid DNA with an excess of HuTOPI and was purified by proteinase K digestion at 37 ºC, phenol/chloroform extraction and ethanol precipitation. After incubation at 37 ºC for 15 min, the reactions were stop by the addition of pre-warmed stop solution (10% SDS/0.5 M EDTA/0.25% bromophenol blue) and electrophoreses on a 1% agarose gel. The DNA was stained with 0.5 μg/mL ethidium bromide and visualized by UV light [25,32].

Molecular modelling: 3D Coordinates of compound **22** and *ct*-DNA for docking analysis was carried according to the method reported earlier [8,25,41,42]. PDBQT formats of ligand files were prepared running for AutoDock 4.2 [42,43]. The 3D affinity grid field with grid map of 96 × 96 × 96 Å were created at grid spacing of 0.375 Å and the center of grid box were 14.71 × 20.97 × 8.82 using auxiliary program Autogrid and placed at the center of DNA structure [44-46]. LGA (Lamarckian gnetic algorthim) were carried out the DNA-target carbazole derivative non-covalent interactions. The lowest energy docked conformation was selected using AutoDock scoring function. The final docked pose obtained by AutoDock were further analyzed using Chimera and PyMol [44-46].

RESULTS AND DISCUSSION

Synthesis of 6-substituted carbazole semicarbazone derivatives **(18-23**) was performed according to **Scheme-I**. Starting material 6-substituted-1,4-dimethyl-9-*H*-carbazole-3-carbaldehydes **(12-17)** synthesized according to the published articles [25,32,36,40]. The equimolar amount of compounds **12-17** [25] and semicarbazide hydrochloride was dissolved in ethanol and refluxed for 4-6 h gve carbazole semicarbazone derivatives (**18-23**). ^{1}H NMR spectra of six target compounds **18-23** showed aromatic protons apperars around at δ 7.0-8.5 ppm, protons for two methyl groups showed singlet peak for each methyl group protons around at δ 2.56 and 2.76 ppm, respectively. The characteristic peaks observed at δ 11.0, 10.0, 8.3 and 6.4 ppm, respectively indicates for indole NH and N-NH, CH=N and NH_2 groups which further confirmed the linking of carbazole to the semicarbazide part [40]. All these exchangeable protons (indole NH and N-NH groups, CH=N and NH_2) completely disappeared in D_2O solvent in proton NMR experiment. ^{13}C NMR spectra of compound **18-23**, peaks for two methyl groups appeared around 16.50 to 16.60 ppm, aromatic carbons in range of 107-140 ppm, Schiff bases characteristic carbon (CH=N) at 156 ppm, carbonyl carbon peak in range of 160 ppm were observed. IR peaks of compound **18-23** using KBr pellet method appeared around for main functional groups at 3435.53, 3312.55 cm^{-1} (NH_2, NH), 3000 cm^{-1}, 2830.37 cm^{-1} (aromatic aliphatic),1673.60 cm^{-1} (C=O), 1595.48 cm^{-1} (C=N) confirms the formation [40]. Further in HRMS mass spectroscopy, the M+1 peak was observed for the compounds (**18** = 281.1401, **19** = 299.1315, **20** = 315.1009, **21** = 359.0501, **22** = 311.1503, **23** = 297.1346 confirming the formation of **18-23**.

TABLE-1
LIPINSKI'S RULE OF FIVE REPRESENTS THE DRUG-LIKENESS OF THE SIX CARBAZOLE SEMICARBAZONES (**18-23**) (ADME PREDICTION)

Compound number	Hepatotoxicity	Cardiotoxicity	Immunotoxicity	Neurotoxicity	Cytotoxicity	LD_{50} (mg/Kg)	BBB-barrier	Class
18	+	-	+	+	-	160	+	3
19	+	-	+	+	-	160	+	3
20	+	-	+	+	-	1260		4
21	+	-	+	+	-	160	+	3
22	+	-	+	+	-	160	+	3
23								

TABLE-2
PREDICTION OF TOXICITIES OF ALL SEX CARBAZOLE SEMICARBAZONES (**18-23**)

Name of compound	m.w. (less than 500 g/mol)	Lipophilicity (less than 5)	TPSA	Hydrogen bond donors (NH or OH) (less than 5)	Hydrogen bond acceptors (N or O) (less than 10)	No. of rule violations (less than 2 violations)	Drug-likeness (Lipinski's rule follows)
18	280.33	3.60	83.28	4	5	0	Yes
19	298.32	2.77	83.28	4	5	0	Yes
20	314.78	4.25	83.28	4	5	0	Yes
21	359.23	4.38	83.28	4	5	0	Yes
22	310.36	3.63	92.51	4	6	0	Yes
23	296.33	3.10	103.50	5	6	0	Yes

ADME and toxicity prediction: Lipinski's rule of five uses to study absorption or permeability of lipid bilayers present in the human body, oral bioavailability of a compound [47]. Molinspiration software was used for prediction of ADME and their results are given in Table-1. Carbazole semicarbazones predicted log P values in a range 2.77-4.38 and its follows Lipinski rule (less than 5). The molecular weights of the carbazole semicarbazones (**18-23**) were less than 500. The numbers of hydrogen-bond acceptor (HBA ≤ 10), for the carbazole semicarbazones (**18-23**) and the hydrogen-bond donor (HBD ≤5) were found to be between 5 and 6, between 4 and respectively. Moreover, it was predicted that all six carbazole semicarbazones would cross the blood–brain barrier (BBB). Protox 3.0 software was used for toxicity prediction for six carbazole semicarbazones (**18-23**) and their results are given in Table-2. All of the compounds were predicted to be class III compounds in terms of toxicity and possessed slight hepatotoxicity and neurotoxicity (six compounds), while most of the compounds were predicted as inactive in terms of cardiotoxicity, mutagenicity and cytotoxicity [47-50]. LD_{50} value of compound **22** was found 160 mg/kg based on protox 3.0 software.

Biological activity

Evaluation of *in vitro* anticancer activity: The results of *in vitro* cytotoxicity (IC_{50}) potential of all the six compounds **18-23** are shown in Table-3. *In vitro* anticancer profile of synthesized compounds **18-23** was found in the order of **22** (OCH_3) > **21** (Br) > **18** (H) > **23** (OH) > **20** (Cl) > **19** (F). Four compounds **18** (R = H), **21** (R = Br), **22** (R = OCH_3), **23** (R = OH) showed better *in vitro* cytotoxicity (IC_{50}) values *viz.* 53.9 ± 10.1 μM, 23.3 ± 4 μM, 13.82 ± 3.86 μM, 58.2 ± 7.6 μM, respectively compared to the standard drug temozolomide (IC_{50} = 100 μM) [25,32]. By changing substitution either electronegative elements like fluoro, chloro, bromo and donating groups on carbazole scaffold were found crucial for potent anticancer activity on U87 MG cell line [24,25,32]. Only compound **22** showed better IC_{50} value that the standard drug carmustine (IC_{50} = 18.24 μM). Further two best cytotoxic compounds (**21** and **22**) also tested on normal cell line (HEK293) using MTT assay showed not cell death at these IC_{50} values on the found on U87MG cell line.

TABLE-3
In vitro ANTICANCER PROFILE OF COMPOUNDS (**18-23**) AND STANDARD ANTICANCER DRUGS

Compound	R	U87 MG cell line IC_{50} (μM)
18	H	53.9 ± 10.1
19	F	198.00 ± 12.5
20	Cl	154.6 ± 10.1
21	Br	23.3 ± 4
22	OCH_3	13.82 ± 3.86
23	OH	58.2 ± 7.6
Temozolomide (Std.)	–	100
Carmustine (Std.)	–	18.24

DNA binding studies

UV-Vis absorption spectral studues: In the UV spectra, a fixed concentration of compound **22** (10 μM) with incremental concentration of the *ct*-DNA solutions (0-20 μM) showed decrease in the absorptivity (hypochromic) at 295 nm respectively without red shift (Fig. 3) Therefore, based on the above observations and supporting literature, compound **22** is likely to interact with DNA through a non-covalent groove-binding mode [11,14,25,32,46].

CD spectroscopy study: The duplex DNA structure with the positive peak at 280 nm and the negative peak at 245 nm

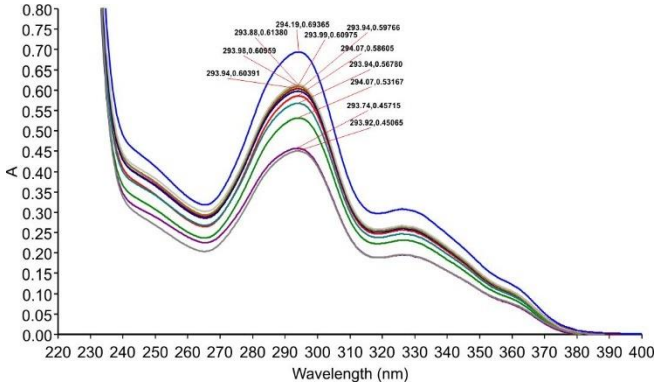

Fig. 3. Electronic absorption spectra of compound **22** (10 μM) with *ct*-DNA (0-20 μM) in the absence [top curve in each] and presence [subsequent curve] of increasing concentration of *ct*-DNA in PBS buffer (pH 7.4) at wavelength 295.44 nm. Arrow shows the absorbance variations upon increasing *ct*-DNA concentration

in CD spectra is related to the double helix structure of B-type DNA [25,32,51,52]. Generally, groove binding molecules with DNA showed less or no major change the intensity of both positive band and negative band in CD spectra [25,51,52].

Various concentrations of compound **22** (10, 20, 30 and 40 μM) with fixed *ct*-DNA concentration (10 μM) scanned in the 240-280 nm region in the CD spectra showed that the intensity of positive band decreased from θ value 2.4 (DNA only) to θ value 1.0 (40 μM), moreover, the bathochromic shift was observed (λ_{max} 272 to λ_{max} 282 nm) in dose dependent manner, however, no major change in the negative band (helicity) was detected (Fig. 4). In this CD experiment, known intercalator ethidium bromide with *ct*-DNA at same concentration ratio (10 μM) enhanced majorly both positive and negative band at 280 and 240 nm wavelength respectively [32]. These results indicated that the regular decrease in the intensity of positive band (stacking) is suggestive of groove binding mode of interaction the compound **22** with *ct*-DNA [32,51-53].

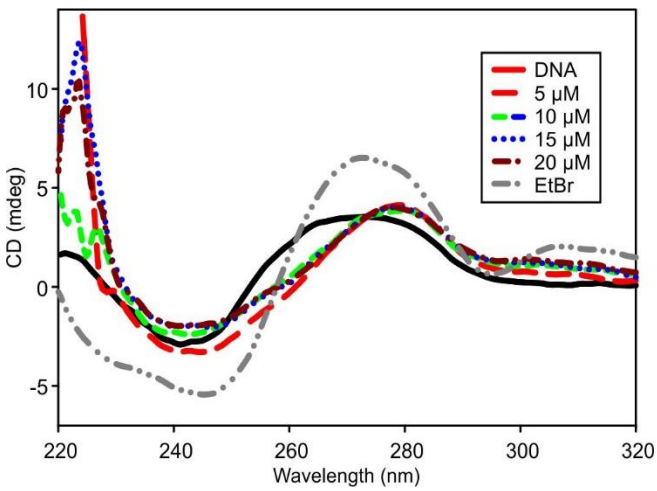

Fig. 4. CD spectra of *ct*-DNA (10 μM) with or without compound **22** (0-20 μM) and known intercalator (10 μM) concentration in PBS buffer (pH 7.4)

Viscosity study: In viscosity study, generally classical intercalators molecules like ethidium bromide showed major increase in the relative viscosity of DNA solution [32]. While, groove binding drugs with DNA showed little positive or negative or no change in the relative viscosity of DNA were observed in literature [54-56]. To evaluate viscosity (η) of *ct*-DNA (50 μM) with various concentrations of the compound **22** (0-50 μM) or standard minor groove binder Hoechst (0-50 μM) respectively were performed using Ostwald viscometer. The values of relative specific viscosity $(\eta/\eta_o)^{1/3}$ *versus* R (R = compound **22**/*ct*-DNA and known groove binder Hoechst/*ct*-DNA) were plotted (Fig. 5). The viscosity of *ct*-DNA with increasing concentration of compound **22** and known minor groove binder Hoechst mainly decreases. This viscosity study showed that compound **22** has groove binding interaction with *ct*-DNA [25,32,54,55,57].

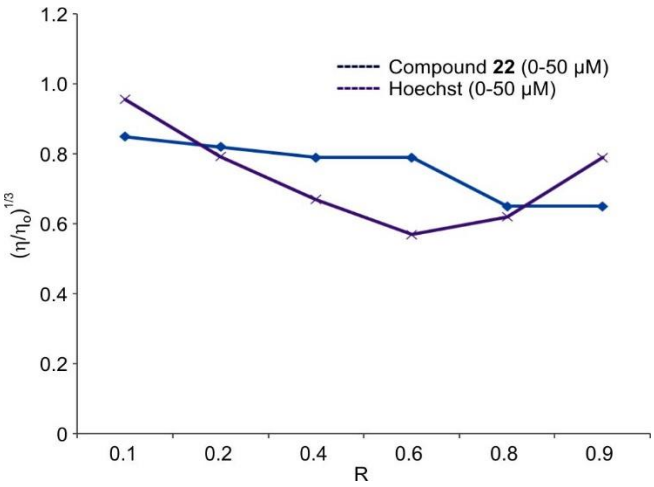

Fig. 5. Study of the relative viscosity of *ct*-DNA (100 μM) with compound **22** (0 to 50 μM) or standard minor groove binder Hoechst (0 to 50 μM) on in PBS buffer (pH 7.4)

Topoisomerase assay and DNA unwinding assay

Effect of compound 22 on topoisomerase assay: The study results found that topoisomerase I converted the supercoiled plasmid DNA molecules (Fig. 6a, lane 1) to their relaxed and partially relaxed forms (lane 2). The relaxation activity of topoisomerase I is not affected with dimethyl sulfoxide solvent (negative control) (lane 3). CPT showed strong topoisomerase I inhibitory activity at 100 μM, which is marked from the recovery of the supercoiled DNA band (lane 4), however no effect on the topo I DNA relaxation activity was observed when 0.01 μM to 100 μM of compound **22** were added to the reaction mixture (lanes 5-8). The topo I activity was found to be inhibited at 50 and 100 μM concentration of compound **22**. Therefore, it is concluded that compound **22** is topo I inhibitor but concentration dependent [25,32,58].

Effect of compound 22 on DNA unwinding assay: The ability of compound to bind the minor groove of DNA was determined by a topoisomerase I-catalyzed unwinding assay, which is based on the ability of intercalating compounds to unwind the DNA duplex and thereby change the DNA twist [25,32,58,59]. Therefore, in the presence of an intercalative compound, a plasmid that is relaxed (*i.e.* contains no superhelical twists) becomes positively supercoiled. Treatment of drug-DNA complexes with mammalian topoisomerase I remove the unconstrained positive DNA superhelical twists that result

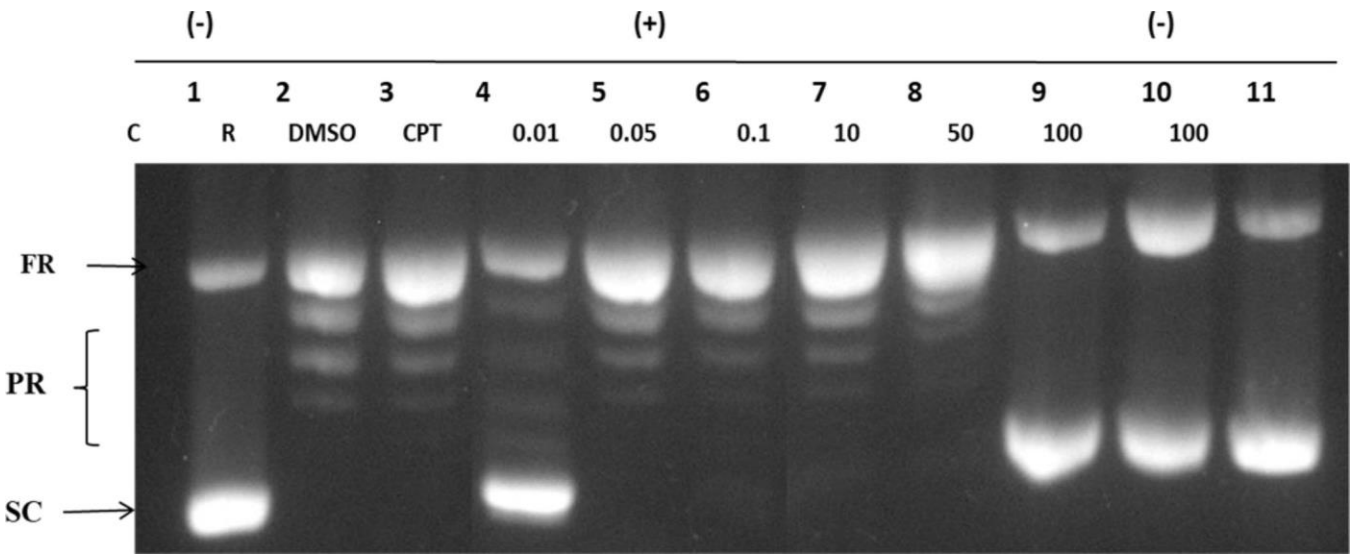

Fig. 6a. An effect of compound **22** on human topoisomerase I. Lane 1, pHOT1plasmid; lane 2, plasmid pHOT1 + human topoisomerase I, 1 units, lane 3 plasmid pHOT1 + DMSO (1%); lane 4, plasmid pHOT1 + Camptothecin (100 µM); lanes 5-10, incubation of plasmid with 0.01 µM to 100 µM of compound **22** for 30 min at 37 ºC with simultaneous addition of 1 units of human topoisomerase I; lane 11, incubation of plasmid with 100 µM of compound **22** without addition of topoisomerase I. FR-fully relaxed, PR- Partially relaxed, SC- supercoiled

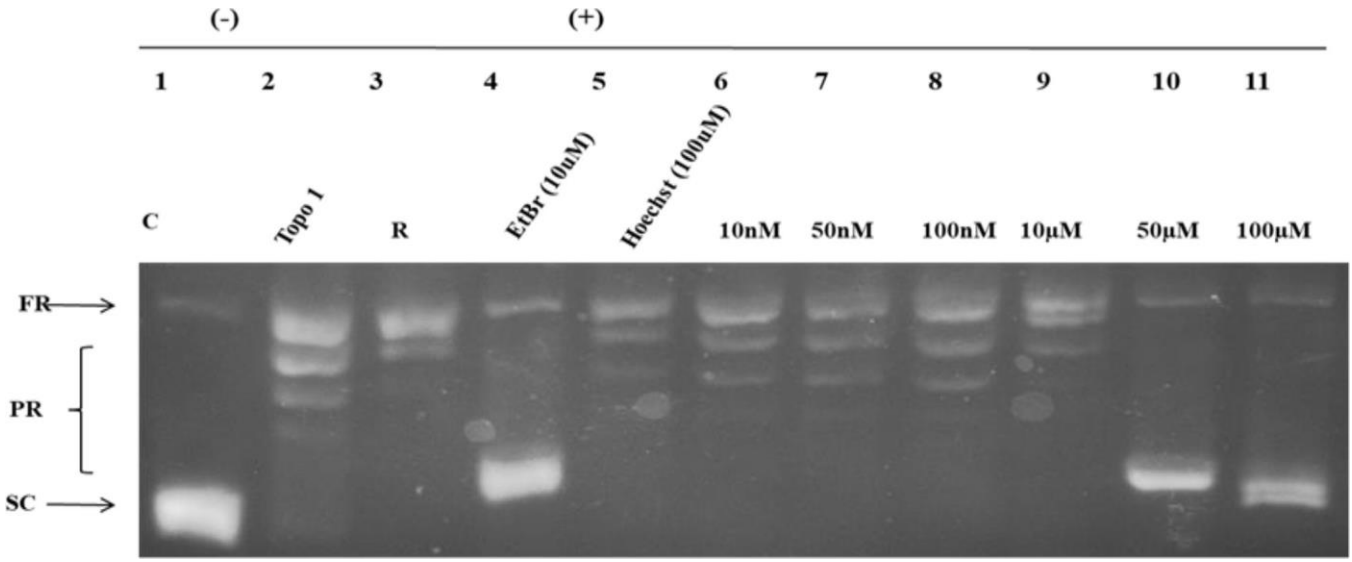

Fig. 6b. Compound **22** with pHOT1 DNA. (a) Lane 1, pHOT1 plasmid DNA (250 ng); lane 2, plasmid pHOT1 + human topoisomerase I, 1 units; lane 3, relaxed pHOT1 plasmid DNA generated by treatment of pHOT1 plasmid DNA (250 ng) with HuTOPI (1U), followed by phenol/chloroform extraction and ethanol precipitation; lane 4, relaxed pHOT1 plasmid DNA + HuTOPI in the presence of 10 µM EtBr; lane 4, relaxed pHOT1 plasmid DNA + HuTOPI in the presence of 100µM of Hoechst 33342; lane 5-10, relaxed pHOT1 plasmid DNA + HuTOPI in the presence of 10 nM, 50 nM, 100 nM, 10 µM, 50 µM and 100 µM of compound **22**, respectively. FR, fully relaxed; PR, partially relaxed; SC, super coiled

from drug intercalation [25,32,58-60]. Following this treatment, extraction of the compound allows the constrained local drug-induced unwinding to redistribute in a global manner and manifest itself as a net negative supercoiling of the plasmid. Thus, in the presence of an intercalative agent such as ethidium bromide, topoisomerase I treatment converts relaxed plasmids to negatively supercoiled molecules. Conversely, when a non-intercalative drug such as Hoechst 33342 is included in reaction mixtures, no DNA super coiling is observed following treatment with the type I enzyme.

As seen in Fig. 6b, supercoiled pHOT1 plasmid DNA (lane 1) was treated with an excess of human topoisomerase I (HuTOPI) such that no supercoiled DNA was left in the reaction mixture (Fig. 6b, lane 3). The relaxed DNA substrate was purified for the unwinding assay. In the presence of ethdium bromide, an intercalating drug, the super coiling of the relaxed substrate DNA was induced at concentrations of 10 µM (lane 4). Conversely, the unwinding of DNA was not observed with the standard minor groove binding drug Hoechst 33342 (100 µM) (lane 5) and with compound **22** at concentration range

of 10 nM to 10 μM (lane 6-9). However, the super coiling of the relaxed substrate DNA was induced at concentrations of 50 μM and 100 μM and this finding provides evidence that compound **22** intercalate into DNA at higher concentrations of 50 μM and 100 μM [60].

Docking analysis: To follow the experimental observations and predict the possible binding mode of compound **22** [(6-methoxy-1,4-dimethyl-9*H*-carbazol-3-yl)methylidene-amino]urea with *ct*-DNA, a docking simulation experiment were performed with AutoDock software [25,32]. The *ct*-DNA sequence d(CGCGAATTCGCG)2 dodecamer (ID: 1BDNA) was obtained from PDB (Protein Data bank) and coordinates were used for docking with the compound **22**. Interactions of compound **22** with *ct*-DNA showed the binding in the minor groove of DNA between A18 to T7 nucleotides sequence (Fig. 7). The docking interaction of compound **22** with DNA showed that the urea moiety in hydrazine carboxamide part of carbazole established two hydrogen bond interactions with DNA, one of the interactions is established with C3′ oxygen of the ribose sugar ring attached to cytosine 9 (C9) base and the second one is interacted with nitrogen bases of adenosine 18 (A18) (Fig. 7). The distance between the hydrogen bonds was found to be 3.5 Å and 3.3 Å respectively. We also observed the 6-methoxy phenyl ring of carbazole in compound **22** interacted with ribose sugar base of thymine 7 (T7) with the bond distance of 3.0 Å. In all cases compound **22** was reside in the minor groove region of DNA with the docking energy -9.81 Kcal mol^{-1}. Intercalator molecule contain planar heterocyclic groups, which stack between adjacent DNA base pairs in molecular docking study. Many minor groove binding drugs also binds to A/T rich region in literature *via* docking results [25,32,52,61-63]. Known groove binder like compound DAPI shows non-covalent interactions between DNA duplex of sequence d (CGCGAATTCGCG) 2 with docking energy -8.8 Kcal mol^{-1} [61-63]. This computational study data showed that compound **22** behave minor groove binder matched with published papers docking results (Fig. 7) [8,25,46,55,64].

Conclusion

In summary, substituted carbazole semicarbazone derivatives (**18–23**) were design, synthesized and characterized. This study represents the first investigation of both the anticancer potential and the *in vitro* DNA-binding properties of carbazole semicarbazone compounds. Among the six derivatives assessed for their *in vitro* cytotoxicity (IC_{50}) against the U87 MG cell line, compound **22** (R = OCH_3) exhibited the most notable activity, with an IC_{50} value of 13.82 ± 3.86 μM, which is superior to that of the standard drug carmustine (IC_{50} = 18.24 μM). In this work, we found changing substitution either electron withdrawing or electron donating group on C6

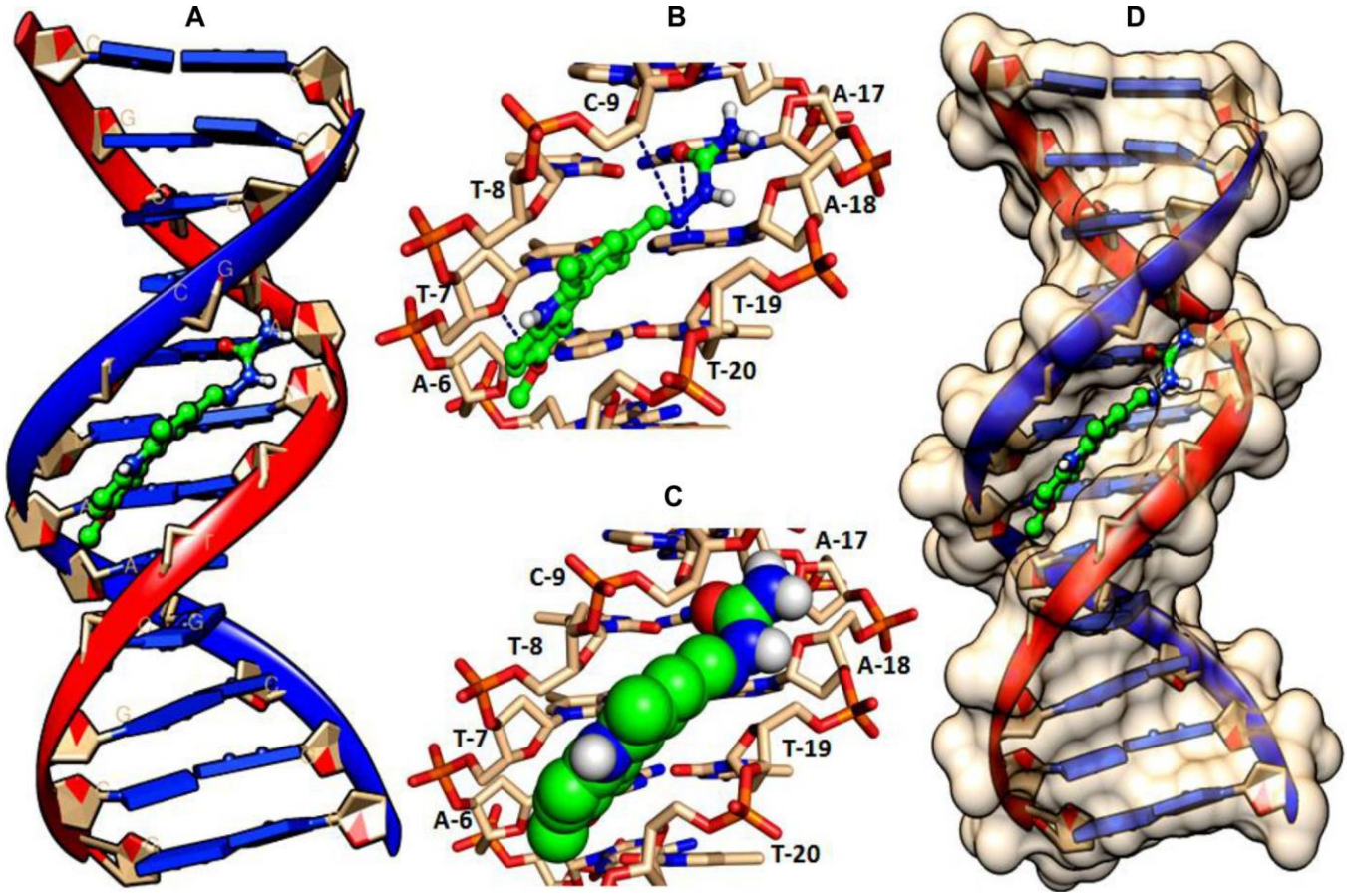

Fig. 7. Compound **22** with *ct*-DNA (d(GTCGACGTCGAC)2), (A) Compound **22**-*ct*-DNA complex (groove region), (B) compound **22** and base pairs shown in ball and stick model. broken lines (Hydrogen bonds-black), (C) Docked compound **22** (green) with *ct*-DNA base pairs are shown with sticks (golden), (D) Compound **22** with *ct*-DNA complex in groove region. Compound **22** is represented in sticks and ball model with atom-based color (green for C, blue for N, and white for H)

position on carbazole semicarbazone structure was crucial for potent anticancer activity on U87MG cell line. In ADME study, carbazole semicarbazone **22** showed log P values 3.63 and its follows Lipinski rule (less than 5). The molecular weights of the carbazole semicarbazone **22** were less than 500. In protox 3.0 data predicted to be class III compound in terms of toxicity and possessed slight hepatotoxicity and neurotoxicity, while inactive in terms of cardiotoxicity, mutagenicity and cytotoxicity. LD_{50} value of compound **22** was found 160 mg/kg based on protox 3.0 software. Thus, it was predicted that carbazole semicarbazones **22** would cross the blood–brain barrier (BBB) based on protox 3.0 software. The interaction of the compound **22** with *ct*-DNA was investigated by UV, CD spectroscopy, viscosity test, topoisomerase assay and docking analysis. All spectroscopic data supports the groove binding behaviour of compound **22** with *ct*-DNA. In viscosity test, decrease viscosity of *ct*-DNA with compound **22** was like well-established groove binding compound Hoechst. In topoisomerase assay, compound **22** also behave groove binding behaviour but it was concentration dependent. Compound **22** (IC_{50} = 13.82 ± 3.86 μM) inhibited Top I enzyme (50 and 100 μM) only. The docking interactions of compound **22** with *ct*-DNA showed the binding in AT rich stretches in the minor groove of *ct*-DNA specifically between A18 to T7 nucleotides sequence. The results illustrated that the 6-methoxy carbazole semicarbazone derivative (compound **22**) interacted with the minor groove of *ct*-DNA and could be used for the development of new effective anticancer agent in the therapy of brain tumors. The next step after *in vitro* evaluation would be to test carbazole semicarbazone compound **22** in appropriate animal models (*e.g.* U87 MG xenograft models) to assess pharmacokinetics, bioavailability, tumor-targeting ability and overall efficacy.

ACKNOWLEDGEMENTS

One of the authors, Pratibha Metha Luthra, is thankful to Department of Science and Technology (DST), Government of India (SR/SO/HS-40/2004) for providing Grant-in-aid to carry this work. The other authors, Nitin Kumar (CSIR- (9/45-(1337)2014-EMR-1 and Neetika Lal, are thankful to C.S.I.R. New Delhi, India, for the providing the scholarship. Another author, Vishal Nemaysh, is thankful to U.G.C., India for the financial support and Centre for Development and Advanced Computing (C-DAC), Bioinformatics Resources and Applications Facility (BRAF), Pune, India. Finally, all the aauthors are also grateful to the USIC (University of Delhi, Instrumentation Facility) for providing ^{1}H NMR,^{13}C NMR and HRMS data.

CONFLICT OF INTEREST

The authors declare that there is no conflict of interests regarding the publication of this article.

REFERENCES

1. S. Hombach-Klonisch, M. Mehrpour, S. Shojaei, C. Harlos, M. Pitz, A. Hamai, K. Siemianowicz, W. Likus, E. Wiechec, B.D. Toyota, R. Hoshyar, A. Seyfoori, Z. Sepehri, S.R. Ande, F. Khadem, M. Akbari, A.M. Gorman, A. Samali, T. Klonisch and S. Ghavami, *Pharmacol. Ther.*, **184**, 13 (2018); https://doi.org/10.1016/j.pharmthera.2017.10.017
2. D.R. Johnson, J.B. Guerin, C. Giannini, J.M. Morris, L.J. Eckel and T.J. Kaufmann, *Radiographics*, **37**, 2164 (2017); https://doi.org/10.1148/rg.2017170037
3. M.A. Patel, J.E. Kim, J. Ruzevick, G. Li and M. Lim, *Cancers*, **6**, 1953 (2014); https://doi.org/10.3390/cancers6041953
4. P.M. Luthra and N. Lal, *Eur. J. Med. Chem.*, **109**, 23 (2016); https://doi.org/10.1016/j.ejmech.2015.11.049
5. A. Shergalis, A. Bankhead III, U. Luesakul, N. Muangsin and N. Neamati, *Pharmacol. Rev.*, **70**, 412 (2018); https://doi.org/10.1124/pr.117.014944
6. R. Stupp, W.P. Mason, M.J. Van Den Bent, M. Weller, B. Fisher, M.J.B. Taphoorn, K. Belanger, A.A. Brandes, C. Marosi, U. Bogdahn, J. Curschmann, R.C. Janzer, S.K. Ludwin, T. Gorlia, A. Allgeier, D. Lacombe, J.G. Cairncross, E. Eisenhauer and R.O. Mirimanoff, *N. Engl. J. Med.*, **352**, 987 (2005); https://doi.org/10.1056/NEJMoa043330
7. S.U. Rehman, T. Sarwar, M.A. Husain, H.M. Ishqi and M. Tabish, *Arch. Biochem. Biophys.*, **576**, 49 (2015); https://doi.org/10.1016/j.abb.2015.03.024
8. I. Ahmad and M. Ahmad, *Int. J. Biol. Macromol.*, **79**, 193 (2015); https://doi.org/10.1016/j.ijbiomac.2015.04.055
9. R. Palchaudhuri and P.J. Hergenrother, *Curr. Opin. Biotechnol.*, **18**, 497 (2007); https://doi.org/10.1016/j.copbio.2007.09.006
10. D. Sahoo, P. Bhattacharya and S. Chakravorti, *J. Phys. Chem. B*, **114**, 2044 (2010); https://doi.org/10.1021/jp910766q
11. S. Ponkarpagam, G. Mahalakshmi, K.N. Vennila and K.P. Elango, *Spectrochim. Acta A Mol. Biomol. Spectrosc.*, **234**, 118268 (2020); https://doi.org/10.1016/j.saa.2020.118268
12. A. Chakraborty, A.K. Panda, R. Ghosh and A. Biswas, *Arch. Biochem. Biophys.*, **665**, 107 (2019); https://doi.org/10.1016/j.abb.2019.03.001
13. N. Ataci, E. Ozcelik and N. Arsu, *Spectrochim. Acta A Mol. Biomol. Spectrosc.*, **204**, 281 (2018); https://doi.org/10.1016/j.saa.2018.06.001
14. S.B. Kou, K.L. Zhou, Z.Y. Lin, Y.Y. Lou, B.L. Wang, J.H. Shi and Y.X. Liu, *J. Biomol. Struct. Dyn.*, **40**, 2908 (2022); https://doi.org/10.1080/07391102.2020.1844057
15. A. Głuszyńska, *Eur. J. Med. Chem.*, **94**, 405 (2015); https://doi.org/10.1016/j.ejmech.2015.02.059
16. P. Luthra and N. Kumar, *Mini Rev. Med. Chem.*, **21**, 2929 (2021); https://doi.org/10.2174/1389557521666210521221808
17. M. Bashir, A. Bano, A.S. Ijaz and B.A. Chaudhary, *Molecules*, **20**, 13496 (2015); https://doi.org/10.3390/molecules200813496
18. C. Asche amd M. Demeunynck, *Anti-Cancer Agents Med. Chem.*, **7**, 247 (2007); https://doi.org/10.2174/187152007780058678
19. R.K. Mongre, C.B. Mishra, A. Prakash, S. Jung, B.S. Lee, S. Kumari, J.T. Hong and M.-S. Lee, *Cancers*, **11**, 1245 (2019); https://doi.org/10.3390/cancers11091245
20. G. Wang, S. Sun and H. Guo, *Eur. J. Med. Chem.*, **229**, 113999 (2022); https://doi.org/10.1016/j.ejmech.2021.113999
21. A. Caruso, M.S. Sinicropi, J.-C. Lancelot, H. El-Kashef, C. Saturnino, G. Aubert, C. Ballandonne, A. Lesnard, T. Cresteil, P. Dallemagne and S. Rault, *Bioorg. Med. Chem. Lett.*, **24**, 467 (2014); https://doi.org/10.1016/j.bmcl.2013.12.047
22. A. Panno, M.S. Sinicropi, A. Caruso, H. El-Kashef, J.-C. Lancelot, G. Aubert, A. Lesnard, T. Cresteil and S. Rault, *J. Heterocycl. Chem.*, **51(no. S1)**, E294 (2014); https://doi.org/10.1002/jhet.1951
23. G.A. Çiftçi, H.E. Temel, Ş.U. Yıldırım, Z.A. Kaplancıklı, M.D. Altıntop and L. Genç, *Med. Chem. Res.*, **22**, 3751 (2013); https://doi.org/10.1007/s00044-012-0325-2
24. N. Kumar, N. Lal, V. Nemaysh and P.M. Luthra, *Asian J. Pharmaceutical Res.*, **14**, 363 (2024); https://doi.org/10.52711/2231-5691.2024.00057
25. N. Kumar, R. Kumar, V. Nemaysh, N. Lal and P.M. Luthra, *RSC Adv.*, **6**, 67925 (2016); https://doi.org/10.1039/C6RA12999D

26. J. Ma, X. Ni, Y. Gao, K. Huang, Y. Wang, J. Liu and G. Gong, *Chem. Pharm. Bull. (Tokyo)*, **67**, 351 (2019); https://doi.org/10.1248/cpb.c18-00738
27. A.C.N. da Cruz, D.J. Brondani, T.I. de Santana, L.O. da Silva, E.F. da O. Borba, A.R. de Faria, J.F.C. de Albuquerque, S. Piessard, R.M. Ximenes, B. Baratte, S. Bach, S. Ruchaud, F.J.B. Mendonça Jr., M.-A. Bazin, M.M. Rabello, M.Z. Hernandes, P. Marchand and T.G. da Silva, *Pharmaceuticals*, **12**, 169 (2019); https://doi.org/10.3390/ph12040169
28. H.-Q. Li, P.-C. Lv, T. Yan and H.-L. Zhu, *Anti-Cancer Agents Med. Chem.*, **9**, 471 (2009); https://doi.org/10.2174/1871520610909040471
29. S. Dutta, S. Padhye, K.I. Priyadarsini and C. Newton, *Bioorg. Med. Chem. Lett.*, **15**, 2738 (2005); https://doi.org/10.1016/j.bmcl.2005.04.001
30. S. Shukla, R.S. Srivastava, S.K. Shrivastava, A. Sodhi and P. Kumar, *Asian Pac. J. Trop. Biomed.*, **2**, S1040 (2012); https://doi.org/10.1016/S2221-1691(12)60358-X
31. S.M. Ali, M.A.K. Azad, M. Jesmin, S. Ahsan, M.M. Rahman, J.A. Khanam, M.N. Islam and S.M.S. Shahriar, *Asian Pac. J. Trop. Biomed.*, **2**, 438 (2012); https://doi.org/10.1016/S2221-1691(12)60072-0
32. N. Kumar, N. Lal, V. Nemaysh and P.M. Luthra, *Bioorg. Chem.*, **100**, 103911 (2020); https://doi.org/10.1016/j.bioorg.2020.103911
33. N. Kumar, V. Nemaysh and P.M. Luthra, *World J. Adv. Res. Rev.*, **16**, 884 (2022); https://doi.org/10.30574/wjarr.2022.16.3.1402
34. M. Gupta, S. Sharma, B.M. Sahoo and B.K. Banik, *Curr. Bioact. Compd.*, **21**, e050624230694 (2025); https://doi.org/10.2174/0115734072298680240521093006
35. M. Stiborová, J. Poljaková, E. Martínková, L. Bořek-Dohalská, T. Eckschlager, R. Kizek and E. Frei, *Interdiscip. Toxicol.*, **4**, 98 (2011); https://doi.org/10.2478/v10102-011-0017-7
36. Y.-J. Xue, M.-Y. Li, X.-J. Jin, C.-J. Zheng and H.-R. Piao, *J. Enzyme Inhib. Med. Chem.*, **36**, 296 (2021); https://doi.org/10.1080/14756366.2020.1850713
37. Ł.J. Walczak and M. Herbet, *Expert Opin. Drug Metab. Toxicol.*, **21**, 1009 (2025); https://doi.org/10.1080/17425255.2025.2520561
38. K. Pavić, I. Perković, M. Cindrić, M. Pranjić, I. Martin-Kleiner, M. Kralj, D. Schols, D. Hadjipavlou-Litina, A.-M. Katsori and B. Zorc, *Eur. J. Med. Chem.*, **86**, 502 (2014); https://doi.org/10.1016/j.ejmech.2014.09.013
39. A.K. Ghosh and M. Brindisi, *J. Med. Chem.*, **63**, 2751 (2020); https://doi.org/10.1021/acs.jmedchem.9b01541
40. G. Bao, B. Du, Y. Ma, M. Zhao, P. Gong and X. Zhai, *Med. Chem.*, **12**, 489 (2016); https://doi.org/10.2174/1573406412666160107113343
41. G.M. Morris, R. Huey, W. Lindstrom, M.F. Sanner, R.K. Belew, D.S. Goodsell and A.J. Olson, *J. Comput. Chem.*, **30**, 2785 (2009); https://doi.org/10.1002/jcc.21256
42. G.M. Morris, D.S. Goodsell, R.S. Halliday, R. Huey, W.E. Hart, R.K. Belew and A.J. Olson, *J. Comput. Chem.*, **19**, 1639 (1998); https://doi.org/10.1002/(SICI)1096-987X(19981115)19:14<1639::AID-JCC10>3.0.CO;2-B
43. M.A. Lill and M.L. Danielson, *J. Comput. Aided Mol. Des.*, **25**, 13 (2011); https://doi.org/10.1007/s10822-010-9395-8
44. V. Nemaysh and P.M. Luthra, *RSC Adv.*, **7**, 37612 (2017); https://doi.org/10.1039/C7RA01305A
45. E.F. Pettersen, T.D. Goddard, C.C. Huang, G.S. Couch, D.M. Greenblatt, E.C. Meng and T.E. Ferrin, *J. Comput. Chem.*, **25**, 1605 (2004); https://doi.org/10.1002/jcc.20084
46. R. Anwer, N. Ahmad, K.I. Al Qumaizi, O.A. Al Khamees, W.M. Al Shaqha and T. Fatma, *J. Mol. Recognit.*, **30**, e2599 (2017); https://doi.org/10.1002/jmr.2599
47. H.A. Alomar, W.M. El Kady, A.A. Mandour, A.A. Naim, N.I. Ghali, T.A. Ibrahim and N. Fathallah, *Results Chem.*, **14**, 102081 (2025); https://doi.org/10.1016/j.rechem.2025.102081
48. F. Merdekawati, *J. Appl. Pharm. Sci.*, **8**, 119 (2018); https://doi.org/10.7324/JAPS.2018.8918
49. M. Agarwal, O. Afzal, Salahuddin, A.S.A. Altamimi, M.A. Alamri, M.A. Alossaimi, V. Sharma and M.J. Ahsan, *ACS Omega*, **8**, 26837 (2023); https://doi.org/10.1021/acsomega.3c01462
50. P. Banerjee, E. Kemmler, M. Dunkel and R. Preissner, *Nucleic Acids Res.*, **52(W1)**, W513 (2024); https://doi.org/10.1093/nar/gkae303
51. J. Lu, Q. Sun, J.-L. Li, W. Gu, J.-L. Tian, X. Liu and S.-P. Yan, *J. Coord. Chem.*, **66**, 3280 (2013); https://doi.org/10.1080/00958972.2013.832228
52. N. Shahabadi, S.M. Fili and F. Kheirdoosh, *J. Photochem. Photobiol. B*, **128**, 20 (2013); https://doi.org/10.1016/j.jphotobiol.2013.08.005
53. J. Kasparkova, O. Vrana, N. Farrell and V. Brabec, *J. Inorg. Biochem.*, **98**, 1560 (2004); https://doi.org/10.1016/j.jinorgbio.2004.04.019
54. N. Akbay, Z. Koksal, T. Taskin-Tok and A. Uzgoren-Baran, *Hacettepe J. Biol. Chem.*, **47**, 177 (2019); https://doi.org/10.15671/hjbc.517481
55. Q. Wang, X. Wang, Z. Yu, X. Yuan and K. Jiao, *Int. J. Electrochem. Sci.*, **6**, 5470 (2011); https://doi.org/10.1016/S1452-3981(23)18421-5
56. M.J. Waring, *Humangenetik*, **9**, 234 (1970); https://doi.org/10.1007/BF00279229
57. N. Shahabadi, S. Kashanian and F. Darabi, *DNA Cell Biol.*, **28**, 589 (2009); https://doi.org/10.1089/dna.2009.0881
58. D.S. Sappal, A.K. McClendon, J.A. Fleming, V. Thoroddsen, K. Connolly, C. Reimer, R.K. Blackman, C.E. Bulawa, N. Osheroff, P. Charlton and L.A. Rudolph-Owen, *Mol. Cancer Ther.*, **3**, 47 (2004); https://doi.org/10.1158/1535-7163.47.3.1
59. Y. Pommier, J.M. Covey, D. Kerrigan, J. Markovits and R. Pham, *Nucleic Acids Res.*, **15**, 6713 (1987); https://doi.org/10.1093/nar/15.16.6713
60. J. Dai, C. Punchihewa, P. Mistry, A.T. Ooi and D. Yang, *J. Biol. Chem.*, **279**, 46096 (2004); https://doi.org/10.1074/jbc.M404053200
61. R. Mishra, A.S. Gaur, R. Chandra and D. Kumar, *Int. J. Pharm. Chem. Anal.*, **2**, 161 (2015).
62. O. Kennard, *Pure Appl. Chem.*, **65**, 1213 (1993); https://doi.org/10.1351/pac199365061213
63. H.K. Srivastava, M. Chourasia, D. Kumar and G.N. Sastry, *J. Chem. Inf. Model.*, **51**, 558 (2011); https://doi.org/10.1021/ci100474n
64. U. Issar, R. Arora and R. Kakkar, *J. Biomol. Struct. Dyn.*, **42**, 4537 (2024); https://doi.org/10.1080/07391102.2023.2220807